

The quasi-resonant variability of the massive LMC system BI 108

Z. Kołaczkowski^{1,2} ^{*}, R.E. Mennickent¹, T. Rivinius³, G. Pietrzyński^{1,4}

¹Universidad de Concepción, Departamento de Astronomía, Casilla 160-C, Concepción, Chile

²Instytut Astronomiczny Uniwersytetu Wrocławskiego, Kopernika 11, 51-622 Wrocław, Poland

³ESO, European Organization for Astronomical Research in the Southern Hemisphere, Chile

⁴Warsaw University Observatory, Al. Ujazdowskie 4, 00-478 Warszawa, Poland.

ABSTRACT

The early B supergiant LMC star BI 108 is photometrically variable with a unique light curve; two strong periods are present in an almost precise 3:2 resonance. We collected spectroscopic data at VLT/UVES, sampling the supercycle of 10.733 days in ten epochs. We find spectral signatures for a SB2 system consisting of two massive B1 supergiants orbiting at the orbital period of 5.366 days. The shorter periodicity resembles the light curve of an eclipsing binary with periodicity 3.578 days that is not detected in the data. We discuss possible causes for the short periodicity and conclude that the quadruple system is the more plausible hypothesis.

Key words: stars: early-type, stars: evolution, stars: binaries: close, stars: variables-others

1 INTRODUCTION

The object LMC SC9-127519 (OGLE 051343.14-691837) was discovered as a variable star with unique photometric properties during our multiperiodicity search in the OGLE-II database (Szymanski 2005). Independently this object was announced as two binary systems in 3:2 resonance by Ofir (2008). With the coordinates, the magnitude ($V = 13.3$) and the color ($B - V = -0.142$), the star was identified as BI 108 in the list of Brunet et al. (1975), for which they give a spectral type of b1-2¹. Schmidt-Kaler et al. (1999) list b1:II: for the same star.

BI 108, in fact a binary or multiple system rather than a single star, is likely one of the brightest members of a young open cluster; NGC 1881 ($\log t < 6.7$, Pietrzyński & Udalski 2000). Although the resonance is not absolutely perfect, such a near resonant and long-term stable period relation is very rare. In order to investigate the photometric behavior of BI 108 all available photometric data were used, as well as a set of 20 UVES observations to determine the spectroscopic behavior. Brief reports of our advances in the understanding of BI 108 were presented in recent conferences (Kołaczkowski et al. 2010; Rivinius et al. 2011).

2 SPECTROSCOPIC OBSERVATIONS AND ARCHIVAL DATA

We secured 20 spectra of BI 108 between October 1, 2008 and January 3, 2009, with the ESO VLT/UVES. The instrument was used in the 437/760 setting, covering most important HeI and Balmer lines and several other transitions of particular interest for hot

stars. At a total of ten epochs two subexposures were taken with $t_{\text{exp}} = 1480$ sec each, with a slit width of 0.8 arcsec, giving an effective resolving power $\lambda/\Delta\lambda$ of about 60 000. The resulting typical S/N is between 90 and 100 for both arms of the instrument.

The UVES standard pipeline ran smoothly on our spectra providing wavelength calibrated 1-D spectra virtually free of instrumental artifacts. The spectra were continuum normalized and heliocentric corrected. The observing log is given in Table 1.

Apart from OGLE-II, data were extracted as well from the MACHO (MACHO object ID 79.5378.25) and the OGLE-III database (Udalski et al. 2008, LMC 111.2.62038). The MACHO data span seven and a half years (HJD 2 448 826.14 to 2 451 541.96), the OGLE-II data almost four years (HJD 2 450 457.76 to 2 451 872.75), and the OGLE-III data over almost eight years (HJD 2 452 167.64 to 2 454 951.52).

The photometric data of all three databases were joined for the analysis. Since the bands are slightly different, this was done the following way: for the time series analysis presented in Sect. 3.1 the mean magnitude was subtracted from each dataset. For the MACHO data, only observations where simultaneous blue and red points exist were accepted. The two measurements were averaged to reduce the individual uncertainty. Note that this combined dataset was *only* used to determine the periods, not for any other analysis. For the actual disentangling of the light curve we chose the OGLE-II data set only, in order to avoid problems due to the different filter bands of each dataset.

3 PHOTOMETRIC PROPERTIES OF THE SYSTEM

3.1 Time series analysis and disentangling

The time series analysis returns two very strong periods, given in Table 2. For reasons that will be shown later, the longer one will be

^{*} E-mail: rmennick@astro-udec.cl. Based on ESO Proposal 382.D-0311

¹ Spectral classes are written in lower-case letters when they have been determined from multicolor photometry.

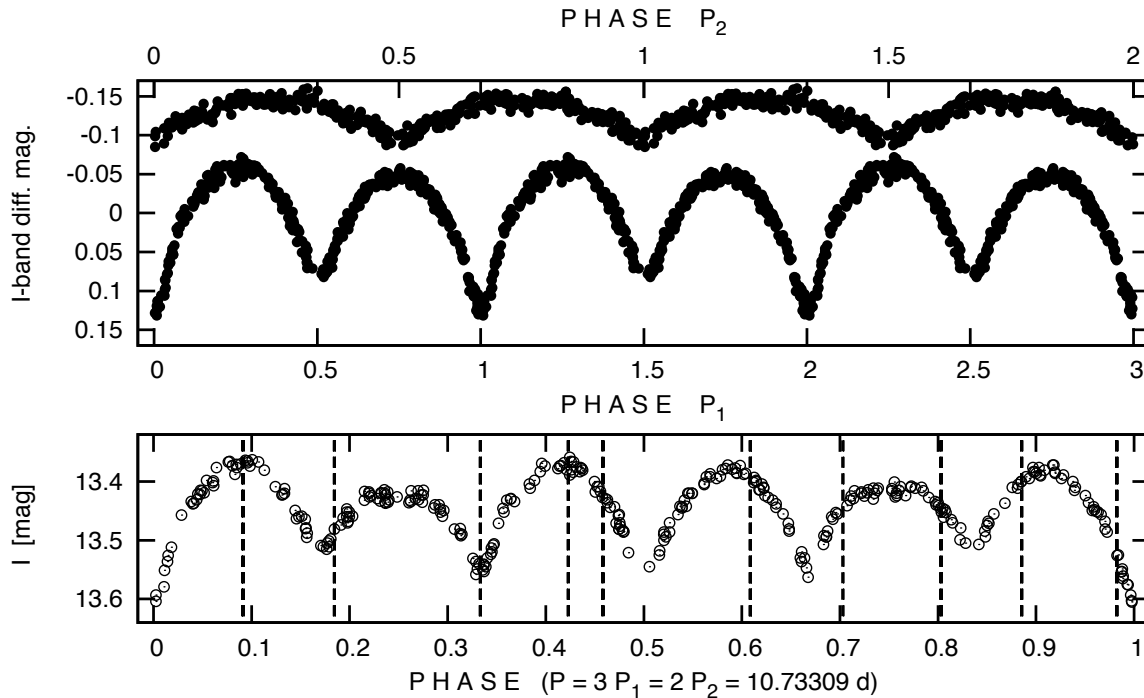


Figure 1. Upper panel: The OGLE-II I-band light curves for both periods of the BI 108 system (upper panel). For each period the contribution of the respective other one has been removed. Lower panel: The original light curve folded with the superperiod. In all cases $HJD_0 = 2\,451\,163.8915$. Dashed lines indicate phases of the spectroscopic observations.

called the orbital period (P_2) and the shorter one the resonant period (P_1). From the light curve alone, however, this is by no means obvious. For none of the two periods is the associated variation sinusoidal in shape, for both the minima are more pronounced and sharper than the maximum associated variations. In fact both variations are of double wave nature.

The stronger variation is associated with the shorter period, $P_1 = 3.577958$ d, with a peak-to-peak amplitude of about 0.18 mag. From the shape alone it is tempting to attribute it to an eclipsing binary nature (Fig. 1, lower curve in the upper panel), however, we will show later that at least spectroscopy shows no sign of any binary with that period.

The longer period shows weaker variations, with about 0.05 mag peak-to-peak, and has the value of $P_2 = 5.366520$ d (Fig. 1, upper curve in the upper panel). In the case of P_2 the two half waves are indistinguishable in photometry, however, and the double wave nature is shown by spectroscopy.

The most interesting feature of both periods is that they have extremely similar superperiods, i.e. they are almost fully resonant with a ratio of $3 : 2$, or $2 \times P_2 = 3 \times P_1 = 10.733$ d. Using the law of propagation of uncorrelated errors we find $P_2/P_1 = 1.499883 \pm 0.000006$. This differs from $3/2 = 1.500000$ by 0.000117 ± 0.000006 , i.e. at the $117/6 = 19.5$ sigma level. The difference between the two superperiods is significant but so tiny, that we will come back to it in the discussion, but ignore it for the rest of this work. Instead, we use our OGLE-II superperiod of 10.73309 d (Rivinius et al. 2011) to analyze variability with the supercycle. The combined light curve phased with that superperiod is shown in the lower panel of Fig. 1. The minima of the combined curve are governed by the stronger variation with P_1 , while P_2 only modulates these minima, i.e. making them more or less

Table 1. Summary of spectroscopic observations discussed in this paper. We adopted $HJD=2\,451\,163.8915$ as epoch for the deepest minimum. All spectra are 1480 s exposures, the dates refer to the beginning of the exposure

Spectrum (label)	HJD (-2450000)	superphase 10.73 d	phase (P_1) 3.58 d	phase (P_2) 5.37 d
BI108-01	4 834.63285	0.0031	0.9318	0.0077
BI108-02	4 834.65057	0.0047	0.9368	0.0110
BI108-03	4 742.76051	0.4434	0.2546	0.8882
BI108-04	4 742.77823	0.4450	0.2595	0.8915
BI108-05	4 746.83997	0.8234	0.3947	0.6483
BI108-06	4 746.85768	0.8251	0.3997	0.6516
BI108-07	4 803.60272	0.1120	0.2593	0.2255
BI108-08	4 803.62044	0.1137	0.2642	0.2288
BI108-09	4 761.66650	0.2048	0.5386	0.4111
BI108-10	4 761.68422	0.2065	0.5435	0.4144
BI108-11	4 796.80764	0.4789	0.3601	0.9594
BI108-12	4 796.82536	0.4806	0.3651	0.9627
BI108-13	4 744.75145	0.6289	0.8110	0.2592
BI108-14	4 744.76917	0.6305	0.8160	0.2625
BI108-15	4 741.79717	0.3536	0.9853	0.7087
BI108-16	4 741.81489	0.3553	0.9902	0.7120
BI108-17	4 745.76182	0.7230	0.0934	0.4475
BI108-18	4 745.77953	0.7246	0.0983	0.4508
BI108-19	4 747.72260	0.9057	0.6414	0.8128
BI108-20	4 747.74031	0.9073	0.6464	0.8161

deep. We choose the date of a deepest minimum as epoch, so that the ephemeris for the superperiod is

$$T_{\text{minlight,super}} = HJD\,2\,451\,163.8915 + E \times 10.73309$$

and the ephemerides for orbital and resonant period are

Table 2. Results of the time series analysis on the combined photometric dataset over 16 years. Amplitudes are MACHO b, MACHO r, and OGLE-II I-band, respectively. The two superperiods, $3 \times P_1$ and $2 \times P_2$, differ by a tiny, yet significant fraction.

	period [d]	superperiod [d]	amplitude [mag]
P_1	3.577958(14)	10.73388(4)	0.172, 0.171, 0.178
P_2	5.366520(8)	10.733040(16)	0.050, 0.047, 0.054

$$T_{\text{minlight},2} = \text{HJD } 2\,451\,163.8915 + E \times 5.366520$$

and

$$T_{\text{minlight},1} = \text{HJD } 2\,451\,163.8915 + E \times 3.577958$$

respectively.

3.2 Stellar parameters

Using $E(B - V) \approx 0.156$ (for NGC 1881, Pietrzyński & Udalski 2000) and the interstellar extinction law derived by Schlegel et al. (1998), we calculated $(B - V)_0 = -0.30$ (indicating b0 II/III, Fitzgerald 1970), $(V - K)_0 = -0.95$, $(J - K)_0 = -0.28$ and $(H - K)_0 = -0.18$ mag. The corresponding figures for a b1 Ib star are -0.19 mag, -0.55 , -0.09 and -0.03 mag, respectively (Fitzgerald 1970; Koornneef 1983). Although variability could affect some of these measurements (though not the MACHO colors, which are taken simultaneously), it is difficult to avoid the conclusion that the infrared colors are bluer than those of a typical b1 (or even b0 or late o type) supergiant.

If we use $V = 13.3$ for the whole system, and assume two equal stellar components, we get $V = 14.05$ for a single star. Using the distance modulus for the LMC of 18.5 mag (Pietrzyński et al. 2009), and the NGC 1881 reddening $E(B - V) = 0.156$ (Pietrzyński & Udalski 2000), we obtain $M_V = -4.96$. Using a bolometric correction of $BC = -2.70$ for a star with $T_{\text{eff}} = 28\,000$ K, $\log g = 3.0$, $v_{\text{turb}} = 10$ km s⁻¹ and $Z/Z_{\odot} = 0.5$ (Lanz & Hubeny 2007), as representative for BI 108, we get an absolute bolometric magnitude of $M_{\text{bol}} = -7.66$. From the evolutionary tracks for $Z = 0.004$ stars by Maeder & Meynet (2001) this luminosity implies a total mass for the system of about $40 M_{\odot}$. The same exercise with four stars gives a total mass of about $60 M_{\odot}$.

The MACHO color term, $B_M - R_M$, does not show any periodic signature, except a signal with a period of 23h56m, i.e. clearly related to Earth's rotation, and apart from this no other variability at all above the statistical error, which is 0.01 mag.

Photometric data were retrieved from 2MASS and Spitzer observational databases and converted to fluxes using the virtual observatory tool VOSA² (Bayo et al. 2008), and compared to published spectral energy distributions. There is no evidence for any IR excess in BI 108, i.e. a significant flux contribution from a cooler component in the visual range is firmly excluded.

4 SPECTROSCOPIC VARIATIONS

4.1 Spectral classification of the components

In the spectra the system obviously has SB2 nature and contains two similar components with spectral features of B1 Ib-II stars. Al-

Table 3. Results to the fit of the combined spectrum at $\Phi_2 = 0.81$.

Parameter	star #1	star #2
T_{eff} [K]	$27\,500 \pm 250$	$27\,500 \pm 250$
$\log g$	3.75 ± 0.05	3.5 ± 0.05
$v \sin i$ [km s ⁻¹]	116 ± 5	116 ± 5
v_{rad} [km s ⁻¹]	401 ± 2	75 ± 2
relat. flux contrib.	1.0 ± 0.02	0.88 ± 0.02

Table 4. System properties of BI 108 derived from the spectroscopic data.

Property	Value	Property	value
q	0.75	$M_1 \sin^3 i$	$19 M_{\odot}$
e	0.08	$M_2 \sin^3 i$	$14.5 M_{\odot}$
ω	93	$M \sin^3 i$	$33.5 M_{\odot}$
$a \sin i$	$41.5 R_{\odot}$		

though both spectra are virtually identical in terms of lines present and $v \sin i$, in the combined light one component produces, on average, slightly weaker lines (and as will be seen from the RV curve is as well less massive). In the following, this star as being the secondary of the current configuration, will be denoted star #2, while the other one will be star #1.

At quadratures the spectral lines are almost separated and can easily be compared to synthetic and other template spectra. A comparison with the B1Ib-II galactic star HD 54 764 gives an almost perfect match between line profiles (even in $v \sin i = 125$ km s⁻¹).

The line ratio HeI 4387/OII 4416 is a useful luminosity indicator.³ The average value is 0.99 ± 0.09 for star #1 and 1.1 ± 0.3 for star-#2, in agreement with a luminosity class I/II derived from the visual classification above.

In spite of what is said above about one star on average being brighter than the other, in some of the quadrature phases the two spectra appear of almost equal strength, i.e. the relative contributions from each star to the equivalent width (EW) are variable. This behavior is discussed in detail below, here it is sufficient to say that the spectral types, understood as defined by spectral line ratios, for instance HeI 4471/MgII 4481, do not change significantly with the variable EW.

In order to obtain individual stellar parameters for both components, the combined spectrum was modeled using the grid of synthetic spectra published by Lanz & Hubeny (2003, 2007)⁴. A multi-parameter fit of those models was done to the UVES data taken at good separation of both components (HJD 2 454 747, $\phi_2 = 0.81$). The fit parameters were effective temperature, surface gravity (in the range $T_{\text{eff}} 25$ kK – 30 kK, $\log g 3 - 4$), radial velocities and $v \sin i$ for each component, as well as the relative flux contribution of secondary component, fixed as unity for the primary (see Table 3). The calculations were done for models with the average LMC metallicities and microturbulence velocities 2 and 10 km s⁻¹. While the hydrogen and helium lines are rather insensitive, the higher microturbulence gives the better fit for the metal lines (Fig. 2).

² <http://www.laefi.inta.es/svo/theory/vosa/>

³ <http://nedwww.ipac.caltech.edu/level5/Gray/frames.html>

⁴ <http://nova.astro.umd.edu/Tlusty2002/tlusty-frames-models.html>

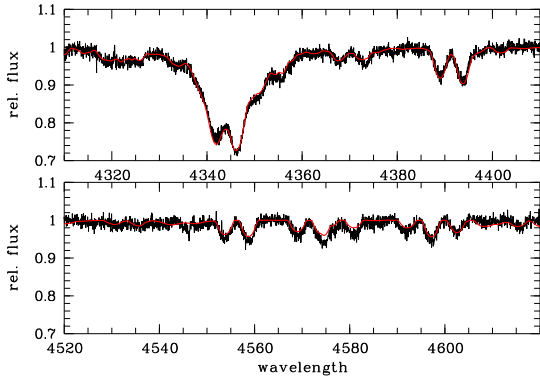


Figure 2. The combined spectrum at $\Phi_2 = 0.81$ along with the best fit whose parameters are given in Table 3.

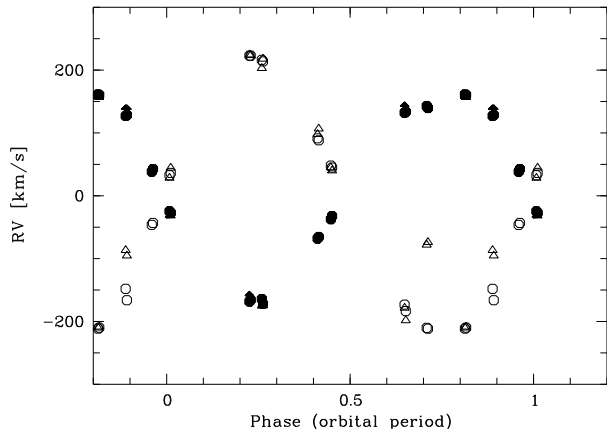


Figure 3. $H\beta$ line (\circ) and SiIII 4553, 4568, 4574 lines (\triangle) radial velocities obtained after Fourier spectral decomposition (filled symbols star #1, open symbols star #2). The two outliers in the secondary's SiIII RVs occur when the spectra are of somewhat lower quality in that region. In other cases, when only one type of symbol is visible this is due to agreement resulting in the two symbols to be plotted above each other. The entire curve is shifted by the γ velocity ($227 \pm 3 \text{ km s}^{-1}$) and centered around 0 km s^{-1} .

4.2 Time series analysis and disentangling

We measured RVs for both components by finding line centers with deblending algorithms, as well by cross correlation of selected spectral regions with templates, but by far the best result was obtained by Fourier disentangling the spectra with the virtual observatory program KOREL⁵ (Hadrava 1995; Škoda & Hadrava 2010). Although robust in spectral disentangling and binary parameter determination, KOREL does not provide the zero point of velocity neither meaningful errors for the system parameters.

The corresponding velocities show that $P_2 = 5.366 \text{ d}$ is clearly a binary orbital period and suggests a near circular orbit (Fig. 3). The period $P_{\text{res}} = 3.577 \text{ d}$ is actually not present in the RVs. The fit for $H\beta$ RVs gives $K_1 = 169 \pm 10 \text{ km s}^{-1}$ and $K_2 = 224 \pm 10 \text{ km s}^{-1}$, i.e. a mass ratio q of about 0.75.

The analysis gives a small non-zero eccentricity of about $e = 0.08$ with a longitude for the periastron of $\omega = 93$ degree.

Similar figures were obtained by using the strongest SiIII lines, providing extra confidence on the above results. While this small eccentricity is compatible with $e = 0.00$ plus non-zero noise, we note the system is relatively young, so a not fully completed circularization is entirely possible. Residual radial velocities, corrected for orbital motion with these parameters, are not sorted with P_1 , i.e. that period does not reflect in the orbital dynamics of the binary system. The entire set of derived parameters is given in Table 4.

We calculated independent system parameters with PHOEBE (Prsa et al. 2011) using the disentangled orbital light curve and assuming $T_1 = T_2 = 27500 \text{ K}$, $P = 5.36654 \text{ d}$, $q = 0.75$, $e = 0$ and no third light. Also we assumed a detached configuration and synchronous rotation of both components. We find $a = 47 R_\odot$, $i = 60.3$ degree, stellar potentials 3.95 and 4.15 for the gainer and donor, respectively. This solution implies $M_1 = 27.7 M_\odot$, $M_2 = 20.8 M_\odot$, $R_1 = 15 R_\odot$, $R_2 = 11.8 R_\odot$. These photometrically derived masses and orbital separation are consistent with the spectroscopic values given in Table 4 for an inclination angle of ≈ 62 degree.

The equivalent widths of lines of both stellar components are highly variable and roughly anticorrelated. The sum of both does vary as well, but with much lower amplitude. Unfortunately, with the available data it cannot be decided whether P_1 or P_2 does sort the data better. Similarly, the line widths are variable (see Fig. 4), with no clear preference for one of the two periods.

5 DISCUSSION

Ofir (2008) originally suggested a quadruple star in (Aa+Ab)+(Ba+Bb) configuration to explain the light curve of BI 108. Similarly, the light curve of CzeV343 was modeled as a double eclipsing binary with periods near a 3:2 ratio (Cagaš & Pejcha 2012). These authors speculate that this resonance might be the result of Kozai cycles and tidal friction during the evolution of a quadruple system, but recognize the lack of theoretical work to confirm this conjecture and that a simple coincidence cannot be discarded. In the case of BI 108, the proximity to perfect resonance is 0.008% (compared with 0.1% for CzeV343) but the circularity of the orbit is in principle inconsistent with Kozai cycles; they tend to increase the ellipticity of central binaries in multiple systems.

For BI 108 the absence of color variations would require the Ba+Bb system has equal components. To make Ba+Bb as dim as possible (in order to hide eventual spectral features), one has to demand that the eclipse in the light-curve is total, such that the entire Ba+Bb subsystem contributes about 20% to the total flux as indicated by the photometric variability. Under such assumptions the individual magnitudes would be 14.3 for Aa and Ab each, and 15.8 for Ba and Bb each, i.e. the subsystem A providing about 80% of the total light in the I -band light curve. Rapid rotation (beyond corotation of the order of 200 km s^{-1}) for both components of Ba+Bb would still be required in order to hide spectral features from this pair from detection in the high S/N data. Taking all the above together, such a quadruple system cannot be ruled out and in spite of the lack of theoretical understanding, this will still turn out to be the hypothesis matching the requirements of Occam's razor.

Another possible multiple system would consist of three stars in non-hierarchical orbits A+B+C, where P_1 is the result of eclipses of the brighter component A by both B and C. Indeed some stable solutions exist for the unrestricted three body problem, for instance those found by Lagrange where three bodies orbit at the vertices of a rotating equilateral triangle. However, this would not only require

⁵ <http://www.asu.cas.cz/had/korel.html>

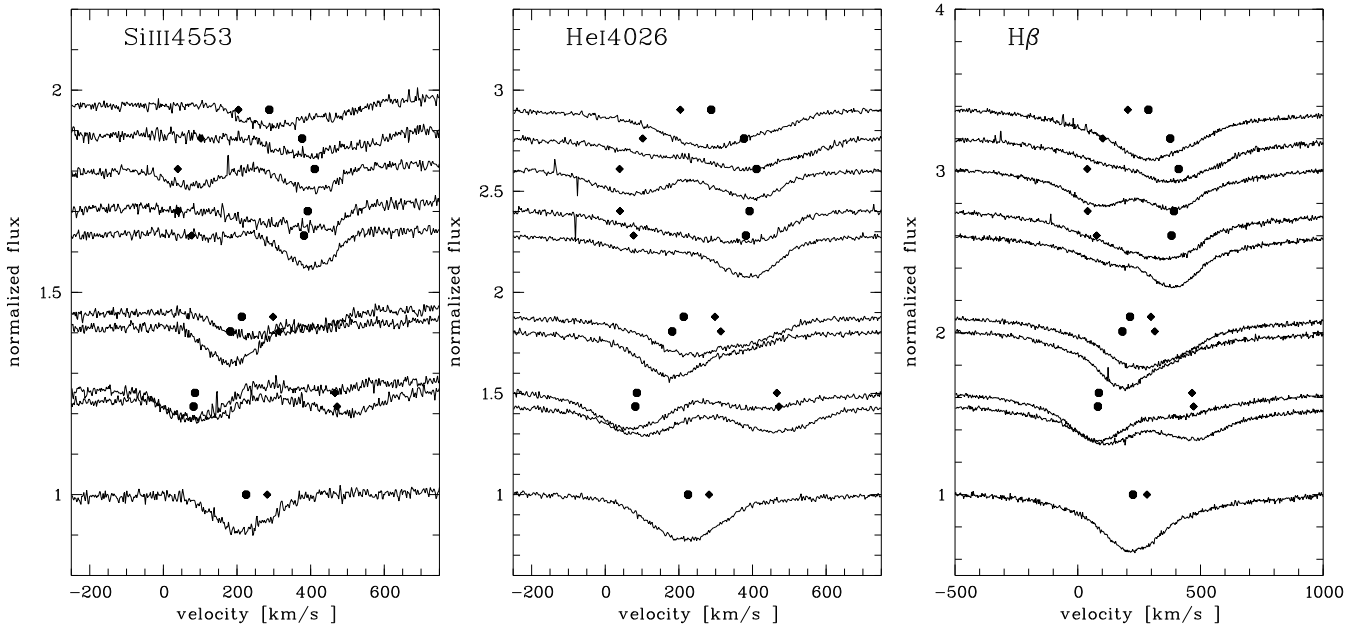


Figure 4. The spectral variability of SiIII 4553, HeI 4026 and H β , sorted with the orbital period, from bottom to top. Offset is proportional to phase and according to values given in Table 1. The RVs as measured in H β are shown as filled disks for star #1 and diamonds for star #2, respectively.

a parameter fine-tuning beyond belief, but probably would still not be stable in a real stellar system undergoing stellar evolution.

If there would be only two stars, they would show variability somehow resonantly synchronized with the orbit. Whatever this mechanism is, to achieve it, the two components must exert force on each other. This could be done through magnetic fields modifying the chemical element distribution on the stellar surfaces, hence producing line and continuum flux variability (Krtićka et al. 2007). Historically, it has been assumed that magnetic fields in OB stars are very rare if not absent. However, according to Petit (2011), “... the increasing discoveries of fields in early B-type stars on the main sequence and pre-main sequence and in both young and evolved O-type stars show convincingly that fossil fields can and do exist in stars with masses as large as 45 solar masses”. However, in BI 108 magnetic fields can be excluded with high probability, due to the missing signatures of chemical inhomogeneities in the spectral lines.

It has been shown that excitation of resonant non-radial g -mode pulsations should be a common phenomenon during tidal evolution of eccentric double main sequence binaries and it is also an effective mechanism for orbital decay (Witte & Savonije 1999, 2001). Although this is a promising mechanism for explaining the P_1 variability in principle, it is difficult to imagine how it could generate the amplitude observed in the P_1 light curve. This would require strongly perturbed stars, the visible stellar surface in the system varying by as much as 20% between maximum and minimum. Thus, other than for the double binary hypothesis, there is a theoretical framework for the variability, however the observed strength of the variation goes far beyond what has been explored in this framework. For this reason we consider it a less likely option than the double binary hypothesis, but note that neither can it be firmly ruled out.

6 CONCLUSIONS

We have presented the first spectroscopic study of the LMC system BI 108 showing an unique 3:2 resonant photometric variability. The immediate goal of the study was to determine which of the two periods (if not both) was due to an eclipsing binary. From the shape of the light-curves, it was originally expected that P_1 would turn out to be the binary period. Surprisingly the radial velocities point to a SB2E system orbiting with orbital period P_2 instead.

The mechanism responsible for P_1 remains unknown, but with the present data we exclude a system with three components and magnetic interaction between two binary components. The 3:2 resonant tidal bulge would require amplitudes beyond what can realistically be expected from such a mechanism. The remaining suggestion, a double binary system seen by chance (or eventually by still unknown dynamical reasons) with a period ratio near 3:2, remains as the most plausible hypothesis.

ACKNOWLEDGMENTS

We acknowledge an anonymous referee for helping to improve a first version of this manuscript. ZK acknowledges support by Polish NCN grant 2011/03/B/ST9/02667. REM acknowledges support by Fondecyt grant 1110347 and BASAL PFB-06/2007. We acknowledge Dr. Moffat for useful comments on a first version of this manuscript. We also thank Igor Soszynski for reading the manuscript and Daniela Barría for running PHOEBE.

REFERENCES

- Bayo A., Rodrigo C., Barrado Y Navascués D., Solano E., Gutiérrez R., Morales-Calderón M., Allard F., 2008, A&A, 492, 277
- Čagaš P., Pejcha O., 2012, A&A, 544, L3
- Fitzgerald M. P., 1970, A&A, 4, 234

- Hadrava P., 1995, *A&AS*, 114, 393
- Kołaczkowski Z., Mennickent R., Rivinius T., 2010, in Prša A., Zejda M., eds, *Binaries - Key to Comprehension of the Universe* Vol. 435 of *Astronomical Society of the Pacific Conference Series*, *The Study of Resonant Variability Observed in the Massive LMC System BI 108*. p. 403
- Koornneef J., 1983, *A&A*, 128, 84
- Krtička J., Mikulášek Z., Zverko J., Žižňovský J., 2007, *A&A*, 470, 1089
- Lanz T., Hubeny I., 2003, *ApJS*, 146, 417
- Lanz T., Hubeny I., 2007, *ApJS*, 169, 83
- Maeder A., Meynet G., 2001, *A&A*, 373, 555
- Ofir A., 2008, *Information Bulletin on Variable Stars*, 5868, 1
- Petit V., 2011, in Neiner C., Wade G., Meynet G., Peters G., eds, *IAU Symposium Vol. 272 of IAU Symposium, Observations of magnetic fields in hot stars*. pp 106–117
- Pietrzyński G., Thompson I. B., Graczyk D., Gieren W., Udalski A., Szewczyk O., Minniti D., Kołaczkowski Z., Bresolin F., Kudritzki R., 2009, *ApJ*, 697, 862
- Pietrzyński G., Udalski A., 2000, *Acta Astron.*, 50, 337
- Prsa A., Matijevic G., Latkovic O., Vilardell F., Wils P., 2011, *Astrophysics Source Code Library*, p. 6002
- Rivinius T., Mennickent R. E., Kołaczkowski Z., 2011, in Neiner C., Wade G., Meynet G., Peters G., eds, *IAU Symposium Vol. 272 of IAU Symposium, The resonant B1III + B1III binary BI 108*. pp 541–542
- Schlegel D. J., Finkbeiner D. P., Davis M., 1998, *ApJ*, 500, 525
- Schmidt-Kaler T., Goehermann J., Oestreicher M. O., Grothues H., Tappert C., Zaum A., Berghöfer T., Brugger H. R., 1999, *MNRAS*, 306, 279
- Szymanski M. K., 2005, *Acta Astron.*, 55, 43
- Udalski A., Szymanski M. K., Soszynski I., Poleski R., 2008, *Acta Astron.*, 58, 69
- Škoda P., Hadrava P., 2010, in Prša A., Zejda M., eds, *Binaries - Key to Comprehension of the Universe* Vol. 435 of *Astronomical Society of the Pacific Conference Series*, *Fourier Disentangling Using the Technology of Virtual Observatory*. p. 71
- Witte M. G., Savonije G. J., 1999, *A&A*, 350, 129
- Witte M. G., Savonije G. J., 2001, *A&A*, 366, 840